TRANSPORTES
revistatransportes.org.br
anpet
associação nacional de pesquisa e ensino em transportes
anpet.org.br

Model predictive control of connected vehicles under automated driving at path-free signal-free intersections

Controle preditivo baseado em modelo de veículos conectados sob condução automatizada em interseções livres de semáforos e com caminhos livres

Elham Ahmadi[1], **Rodrigo Castelan Carlson**[1]

[1]Federal University of Santa Catarina, Florianópolis, Santa Catarina, Brasil
Contact: elham.ahmadi@posgrad.ufsc.br, (EA); rodrigo.carlson@ufsc.br, (RCC)

Submitted:
3 June, 2022
Accepted for publication:
2 June, 2023
Published:
12 December, 2023

Associate Editor:
Flávio José Craveiro Cunto, Universidade Federal do Ceará, Brasil

Keywords:
Traffic control.
Connected vehicles under automated driving.
Model predictive control.
Urban intersections.

Palavras-chave:
Controle de tráfego.
Veículos conectados sob condução automatizada.
Controle preditivo baseado em modelo.
Interseções urbanas.

DOI: 10.58922/transportes.v31i3.2880

OPEN ACCESS
CC BY

ABSTRACT
In this paper, we tackle the problem of real-time multi-vehicle interactions at signal-free and path-free intersections, which we call plazas, aiming for an efficient use of the intersection space. We propose a method that combines the path planning and path following tasks of connected vehicles under automated driving in one formulation. The method extends the standard nonlinear model predictive contouring control for application at intersections via the generation of multiple time-independent reference paths. The goal is to maximize the progress of each vehicle along its reference path and penalize the rate of the control inputs while handling the continuous arrivals of the vehicles. The method is demonstrated using numerical simulation of vehicles at an intersection. The simulation results show that the proposed method achieves optimal and safe trajectories of the vehicles with driving flexibility and the possibility of better utilizing the intersection space.

RESUMO
Neste artigo, aborda-se o problema de interações em tempo real de múltiplos veículos em interseções livres de semáforos e com caminhos livres, denominadas de plazas, para um uso eficiente do espaço da interseção. Propõe-se um método que combina o planejamento e seguimento de caminhos de veículos conectados sob condução automatizada em uma formulação. O método estende o controle de contorno preditivo não linear baseado em modelo padrão para aplicação em interseções por meio da geração de múltiplos caminhos de referência independentes do tempo. O objetivo é maximizar o avanço de cada veículo ao longo do seu caminho de referência e penalizar as entradas de controle enquanto os veículos chegam continuamente. O método é demonstrado por simulação numérica de veículos em uma interseção. Os resultados mostram que o método proposto obtém trajetórias ótimas e seguras para os veículos, com flexibilidade de condução e possibilidade de melhor aproveitamento do espaço da interseção.

1. INTRODUCTION

Connected vehicles under automated driving (CVAD) have the potential to improve both traffic safety and traffic efficiency at intersections. The CVAD approaching an intersection have a good perception of the road infrastructure, of other CVAD, and of traffic participants. Moreover, the CVAD are capable of exchanging information with the infrastructure and/or other CVAD. They enable autonomous intersection management (AIM) with the elimination of the traffic light cycle. There is extensive research on intersection modeling for AIM (Chen and Englund, 2015, Rios-Torres and Malikopoulos, 2016), including space and time discretization (Schepperle and Böhm, 2009), paths modeling (Lee and Park, 2012), and conflicting regions/points modeling (Müller, Carlson and Kraus Jr, 2016a; 2016b). Although traffic efficiency was increased with these approaches by enabling shorter headway and by eliminating lost time, the intersection's capacity is limited by the relationship between pre-established paths.

Exploiting the whole intersection space can be achieved by utilizing the CVAD's potential to enable path-free traversing of a signal-free intersection, i.e., without being bound to predefined paths. This allows for smaller headways between vehicles and eliminates unnecessary stops at intersections. Similar ideas have been proposed for the related lane-free traffic approach. Papageorgiou et al. (2021) introduced a lane-free traffic model known as TrafficFluid, which is based on two principles, lane-free traffic and vehicle nudging. The former is the possibility for vehicles to drive on roads without being bound to lanes, while the latter is the communication of the presence of vehicles to other vehicles in front of them.

For intersections, Li et al. (2018) proposed a motion planning method for connected automated vehicles (CAVs) crossing a lane-free intersection via a two-stage centralized control strategy. First, CAVs reach a standard intersection formation that is performed online, and then an offline optimal control problem (OCP) is used to coordinate the vehicles crossing the intersection. However, this problem is numerically intractable and computationally expensive due to the high-dimensional collision avoidance constraints and nonlinearity of the model. Li et al. (2020) simplified the problem by fixing the time that a vehicle takes to traverse the intersection and via modification of the collision-avoidance constraints. These works evolved into a batch-processing framework for autonomous intersection management that is an integration of planning and reservation methods (Li et al., 2021). The former handles the batches macroscopically, and the latter optimizes the cooperative trajectories in one batch microscopically.

Another work considers path-free signal-free intersection modelling, which is called a plaza (Ahmadi et al., 2021). The vehicles exploit the full intersection space including the usage of the opposite road lanes without movement-related horizontal markings, except for the intersection boundaries. This could increase the average inter-vehicle spacing, thus allowing for higher flow and capacity, because otherwise unoccupied intersection spaces would be used for completing trips. Two methods were proposed for near-optimal coordination of the CVAD at the plaza by (Ahmadi et al., 2021; 2022), one based on finite Fourier series (FFS), and one based on Bézier curves. In both methods, only the state variables of each CVAD are interpolated and control variables are considered in the objective function. The use of the FFS and Bézier methods converts the intersection trajectory optimal control problem to a nonlinear programming (NLP) problem. The numerical results demonstrated that the

proposed methods could generate near-optimal trajectories for CVAD. Similarly, Amouzadi, Orisatoki and Dizqah (2022) formulated the lane-free crossing of CAVs through signal-free intersections as a nonlinear minimum-time optimal control problem. The proposed formulation used the dual problem theory for smoothing the non-convex and non-differentiable collision avoidance constraints between CAVs and between CAVs and road boundaries. They showed that the resulting smoothed OCP could reduce the crossing time significantly compared to a space and time discretization strategy. However, the nonlinear OCP methods presented by Ahmadi et al. (2021; 2022) and Amouzadi, Orisatoki and Dizqah (2022) do not consider the continuous arrival of vehicles, are off-line, and force the CVAD to have the same completion times, thus not addressing a realistic problem.

To tackle the limitation of the previous works, Carlson et al. (2022) and Ahmadi and Carlson (2022) proposed an optimization-based receding horizon approach. Carlson et al. (2022) formulated the coordination of CVAD in path-free signal-free intersections as a non-linear model predictive control which is an extension of a model predictive controller for path and trajectory planning on roads without lanes proposed by Levy and Haddad (2021) (see also the work by Levy and Haddad (2022)). They compared their method with the optimal time scheduling strategy which uses a predetermined number of paths (Müller, Carlson and Kraus Jr, 2016a; 2016b) and showed a better use of the intersection space. Ahmadi and Carlson (2022) formulated the trajectory optimization problem of the CVAD at path-free signal-free intersections as a nonlinear model predictive contouring control (NMPCC) problem (Liniger et al., 2015, Lam, Manzie and Good, 2010, Romero et al., 2022, Schwarting et al., 2017, Levy and Haddad, 2022). The standard NMPCC was extended and tailored for solving trajectory optimization problems in intersection applications. The controller maximizes the progress of all CVAD at the intersection with minimal control efforts under different types of constraints, such as vehicle model, intersection geometry layout, and so on. In this work, we expand the preliminary work of Ahmadi and Carlson (2022) by the use of a different vehicle kinematic model that does not have rear-wheel driving, differing from the previous works, and by presenting more detailed results. The used model allows us to design more accurate collision avoidance constraints, especially between CVAD. The proposed NMPCC controller generates real-time collision-free and optimal CVAD trajectories based on time-independent and continuously differentiable reference paths in which the progress along the path is maximized. In addition, we investigate the performance of the proposed controller in more detail. We summarize the contributions of this paper as follows:

- The development of a real-time NMPCC suitable for optimal trajectory generation of CVAD in an intersection plaza.
- Generation of multiple reference paths that cover all possible movements including straight and turning movements in an intersection.
- Introduction of practical collision avoidance and boundary constraints to avoid collisions between CVAD and with the intersection boundaries.
- Simulation of a realistic traffic scenario with different driving movements and with continuous arrivals of CVAD in the intersection.

In Section 2, we describe the Nonlinear Model Predictive Contouring Control Problem (NMPCC). In Section 3, we show how we use the NMPCC for the coordination of CVAD at

a signal-free path-free intersection. The simulation results are demonstrated in Section 4. The conclusions are presented in Section 5.

2. MODEL PREDICTIVE CONTOURING CONTROL PROBLEM

This section provides a summary of the original NMPCC algorithm based on the work by Lam et al. (2010).

2.1. Preliminaries on model-based predictive control

In Model-based Predictive Control (MPC) (Rossiter, 2018), the goal is to use a model of the system to predict the system's output for a number of time steps in the future while minimizing an objective function that defines the distance between the predicted outputs and some given desired outputs. This problem is a reference tracking problem since at each sampling time the outputs of the system are forced to track a reference signal at a certain time. A key advantage of the MPC is that the constraints can be explicitly considered in the optimal control problem. By solving the corresponding optimal control problem, a sequence of control inputs is obtained. However, only the first control input is applied to the system and the optimization is repeated. The number of time steps ahead utilized for prediction is called the prediction horizon. When the involved model, objective function and/or constraints are non-linear, the control problem becomes a Non-linear Model-based Predictive Control (NMPC).

2.2. The contouring control problem

In the contouring control problem, the control objective is the minimization of the contouring error, which is the minimum distance between the current position of an object or a tool and its reference while maximizing the progress along a reference path. In path following control, the controller determines the velocity of the reference path as well as the control inputs online. A path following control framework based on MPC (MPFC) was proposed by Faulwasser et al. (2009). Then, Lam et al. (2010) extended the MPFC to the contouring control problem, which is called the non-linear model predictive contouring control problem (NMPCC).

NMPCC solves a path following control problem (Faulwasser, Kern and Findeisen, 2009) in which the goal is to follow a reference path as fast as possible with minimal error. This is equivalent to maximize the progress while minimizing the distance to the reference path. The advantage of the NMPCC is that both path planning and path tracking can be combined in a single nonlinear optimization problem by using the ideas of contouring control (Lam, Manzie and Good, 2010).

It is important to note the difference between tracking and path following. In tracking, each object is required to track a time-parametrized reference trajectory and to reduce tracking error, i.e., the difference between the reference and measured output. In path following, the objects are only required to travel along the desired path without the need of tracking precisely the time-parametrized reference trajectory.

2.3. Dynamic model

The dynamic model of the object to be controlled is described by the following discrete time system:

$$\boldsymbol{z}_{k+1} = f(\boldsymbol{z}_k, \boldsymbol{u}_k), \tag{1}$$

with $f(\cdot)$ a nonlinear function that defines the dynamic of the system, $\boldsymbol{z}_k$ the state vector, $\boldsymbol{u}_k$ the vector of control inputs, k the discrete time index such that $t = k\,\Delta t$, and Δt the sampling time.

2.4. Progress on a reference path using parametrization

The reference path $(x^{\mathrm{ref}}(\theta), y^{\mathrm{ref}}(\theta))$ is parameterized by its arc length θ. The parameterization of curves by arc length is nontrivial, however, there are interpolation methods like splines to approximate the arc length (Lam, Manzie and Good, 2010). The approximated progress of the object is described as:

$$\theta_{k+1} = \theta_k + \Delta t\, \nu_k, \nu_k \in [0, \nu_{\max}], \nu_{\max} > 0, \tag{2}$$

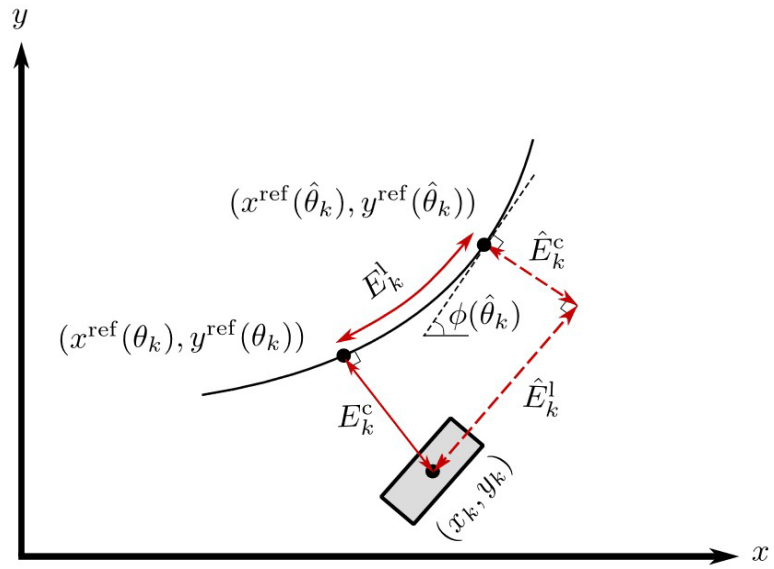


Figure 1: Reference path, contouring error, lag error and their approximation.

with θ_k the path parameter that shows the arc length of the reference path, ν_k a virtual input that controls the evolution of θ_k, and $\nu_{\max}$ a maximum value for the virtual input. The solid black curve in Figure 1 shows a reference path. In fact, Equation 2 approximates the evolution of the path parameter by the travelled distance of the object.

2.5. Contouring and lag errors

The contouring error, which is the shortest distance of the actual position of the object (x_k, y_k) from the reference path at θ_k, $(x^{\mathrm{ref}}(\theta_k), y^{\mathrm{ref}}(\theta_k))$, see Figure 1. Since calculating this distance is computationally expensive, an approximation is introduced for the contouring error as follows:

$$\hat{E}_k^{\mathrm{c}} = \sin\left(\phi(\hat{\theta}_k)\right)\left(x_k - x^{\mathrm{ref}}(\hat{\theta}_k)\right) - \cos\left(\phi(\hat{\theta}_k)\right)\left(y_k - y^{\mathrm{ref}}(\hat{\theta}_k)\right), \tag{3}$$

and $\phi(\hat{\theta}_k) = \arctan\left(\frac{\nabla y^{\mathrm{ref}}(\hat{\theta}_k)}{\nabla x^{\mathrm{ref}}(\hat{\theta}_k)}\right)$.

Let us denote θ_k as the value of path parameter where the distance between the point (x_k, y_k) and $(x^{\text{ref}}(\theta_k), y^{\text{ref}}(\theta_k))$ is minimal, see Figure 1. However, considering the fact that calculating θ_k is an optimization problem itself, let us denote $\widehat{\theta}_k$ as an approximation to θ_k. To make this approximation applicable, it is necessary to link the actual path parameter θ_k and its approximation $\widehat{\theta}_k$ by introducing the lag error, which is the difference between θ_k and $\widehat{\theta}_k$ (see Figure 1):

$$\hat{E}_k^{\text{l}} = -\cos\left(\phi(\hat{\theta}_k)\right)\left(x_k - x^{\text{ref}}(\hat{\theta}_k)\right) - \sin\left(\phi(\hat{\theta}_k)\right)\left(y_k - y^{\text{ref}}(\hat{\theta}_k)\right), \tag{4}$$

and $\phi(\hat{\theta}_k)$ as defined before.

2.6. Cost function

The objective of the NMPCC problem is to minimize the contouring and lag errors while maximizing the progress along the reference path. Given $\widehat{\boldsymbol{E}}_k = \left[\hat{E}_k^{\text{c}}, \hat{E}_k^{\text{l}}\right]^T$, the NMPCC cost function is defined as:

$$J_{\text{NMPCC}} = \sum_{k=0}^{N-1} \widehat{\boldsymbol{E}}_k^T \, Q \widehat{\boldsymbol{E}}_k + v_k^T \, r_{\text{v}} \, v_k - q_\theta \hat{\theta}_k, \tag{5}$$

with N the prediction horizon, and

$$Q = \begin{bmatrix} q_{\text{c}} & 0 \\ 0 & q_{\text{l}} \end{bmatrix}, q_{\text{c}}, q_{\text{l}}, q_\theta > 0, r_{\text{v}} > 0, \tag{6}$$

where q_{c}, q_{l}, r_{v}, and q_θ are the contouring error, the lag error, the virtual input, and the progress cost weights, respectively. A suitable tuning of these weights might provide a good trade-off between contouring accuracy and maximum progress.

3. METHOD

In this section, we introduce the extended NMPCC (E-NMPCC) method and make it applicable to CVAD path and trajectory optimization at the intersection plaza. In our problem, compared to the standard NMPCC, there are multiple objects involved, the CVAD on the intersection, and multiple reference paths, corresponding to the possible origin-destination pairs. In addition, we introduce the intersection modeling, practical safety constraints, and a performance index. We also consider the continuous arrivals of multiple CVAD at the intersection plaza.

3.1. Intersection plaza modelling

We select a four-leg intersection depicted in Figure 2 to introduce our concept. The figure illustrates an example layout of a plaza, shown by the yellow area, in which a vehicle is traversing from its initial position, depicted by a dark rectangle, toward its destination shown by the light gray rectangle. The vehicle is free to adjust its trajectory, shown by the solid red line, without being bound to predetermined paths while remaining inside the red circles to avoid collision with the intersection boundaries.

The x and y axes represent the central lines of the intersection on the Cartesian coordinate system. We use the center lines of the roads as reference paths that should be followed by the CVAD. For the intersection in Figure 2, we generate four different road

center-lines as the reference paths, to cover through and left or right turning movements of the CVAD as shown by the colored dashed lines in the figure. Each reference path is then followed by a particular vehicle according to its traversal intention at the intersection. As an example, the light blue dashed line shows the reference path for the vehicles approaching the plaza from the west intending to make a left turn. The remaining reference paths have the same description for other directions. Note that we just use the reference paths for measuring the progress and for controlling the contouring error.

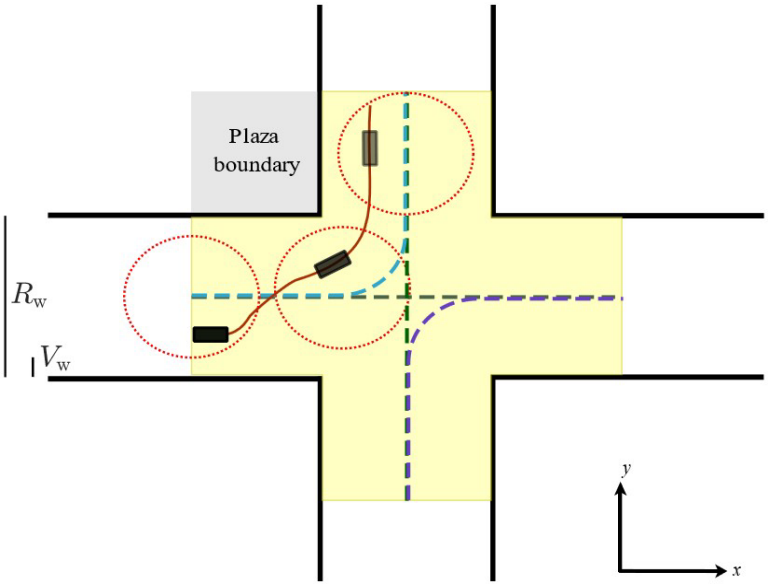


Figure 2: A four-leg intersection as a plaza (yellow area).

3.2. Vehicle model

We model each vehicle i within the intersection plaza by using a nonlinear kinematic bicycle model. This model falls the left and right wheels into a pair of single wheels at the middle of the vehicle's axles, see Figure 3. The equations of motion are described by the following state equations (Polack et al., 2017):

$$\begin{aligned} \dot{x}_i(\mathrm{t}) &= v_i(t)\cos\left(\psi_{\mathrm{i}}(t)+\beta_{\mathrm{i}}(\mathrm{t})\right), \\ \dot{y}_i(t) &= v_i(t)\sin\left(\psi_i(t)+\beta_i(t)\right), \\ \dot{\psi}_i(\mathrm{t}) &= \frac{v_i(t)\sin\left(\beta_i(t)\right)}{l_{\mathrm{r}}} \\ \dot{v}_i(t) &= u_i^1(t), \\ \beta_i(t) &= \tan^{-1}\left(\frac{l_{\mathrm{r}}}{l_{\mathrm{f}}+l_{\mathrm{r}}}\tan u_i^2(t)\right), \end{aligned} \tag{7}$$

where $i = 1, \ldots, M$, with M the number of CVAD at the plaza. The i-th vehicle state vector is denoted by $\boldsymbol{z}_i = [x_i, y_i, \psi_i, v_i]^T$ in which x and y are the longitudinal and lateral position of the CVAD, respectively, ψ is the orientation angle, and v is the speed at center of gravity (CG) of the vehicle, as seen in Figure 3. The control input vector is denoted by $\boldsymbol{u}_i = [u_i^1, u_i^2]^T$, in which u_i^1 and u_i^2 are the acceleration (a_i) and steering angle (δ_i) of the vehicle,

respectively. The distance from the CG of the vehicle to the front and rear axles are denoted, respectively, as l_{f} and l_{r}. The model in Equation 7 is discretized with sampling time Δt by using Euler discretization, and augmented with Equation 2 to consider the progress of the vehicles along the reference path:

$$\begin{aligned} x_{i,k+1} &= x_{i,k} + \Delta t\, v_{i,k} \cos\left(\psi_{i,k} + \beta_{i,k}\right), \\ y_{i,k+1} &= y_{i,k} + \Delta t\, v_{i,k} \sin\left(\psi_{i,k} + \beta_{i,k}\right), \\ \psi_{i,k+1} &= \psi_{i,k} + \Delta t\, \frac{v_{i,k}\, \sin\left(\beta_{i,k}\right)}{l_{\mathrm{r}}}, \\ v_{i,k+1} &= v_{i,k} + \Delta t\, u^{1}_{i,k}, \\ \widehat{\theta}_{i,k+1} &= \widehat{\theta}_{i,k} + \Delta t\, \nu_{i,k}. \end{aligned} \tag{8}$$

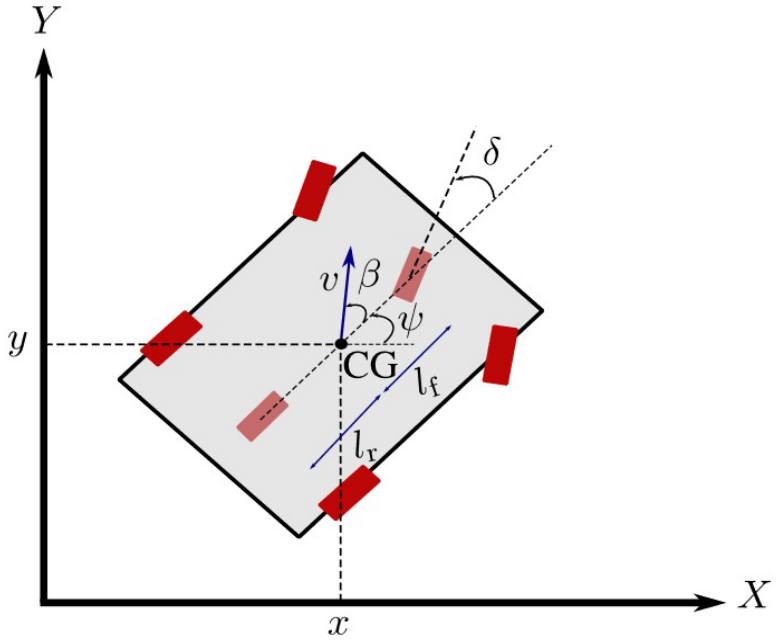


Figure 3: Kinematic bicycle model with x and y the longitudinal and lateral position of each CVAD.

The vehicle model in Equation 8 is a nonlinear dynamic system in the form of Equation 1 and is used in the E-NMPCC formulation. In Equation 8, the progress and the virtual input are considered as an additional state variable and an additional control variable, respectively. To guarantee that the vehicles are within their dynamic limitations, the following constraints are imposed for each CVAD:

$$\begin{aligned} v_{\min} \leq v_{i,k} \leq v_{\max}, \\ \delta_{\min} \leq \delta_{i,k} \leq \delta_{\max}, \\ a_{\min} \leq a_{i,k} \leq a_{\max}, \end{aligned} \tag{9}$$

where $v_{\min}$, $v_{\max}$, $\delta_{\min}$, $\delta_{\max}$, $a_{\min}$, and $a_{\max}$ are the lower and upper bounds of speed, steering angle, and acceleration, respectively.

Finally, it should be noted that the the vehicle model in Equation 8 is an appropriate choice for the application in this work (Polack et al., 2017). Moreover, the vehicle model in Equation 8 does not have rear-wheel driving, in contrast to the vehicle model used by

Ahmadi and Carlson (2022) and Carlson et al. (2022). In this model, the speed and the orientation angle are considered at the CG of the vehicle, see Figure 3. This allows for a more accurate model when defining collision avoidance constraints.

3.3. Vehicle-to-vehicle collision avoidance constraints

To avoid collisions between the CVAD, a minimum safe distance, d_{s}, must be kept in any direction between every two vehicles:

$$\mathrm{dist}\big(\mathrm{CVAD}_i, \mathrm{CVAD}_j\big) \geq d_{\mathrm{s}} + L_{\mathrm{v}}, \tag{10}$$

in which $\mathrm{dist}\big(\mathrm{CVAD}_i, \mathrm{CVAD}_j\big)$ is the Euclidean distance between vehicles i and j, $i, j = 1, \dots, M$, $i \neq j$, and L_{v} is the vehicle length.

3.4. Plaza boundaries constraints

In addition to avoiding collisions between vehicles, a set of constraints must be enforced to prevent that CVAD violate the boundaries of the plaza. To do so, each vehicle is allowed to traverse only inside a well-defined circle whose center point is $p^{\mathrm{ref}} = (x^{\mathrm{ref}}(\hat{\theta}_k), y^{\mathrm{ref}}(\hat{\theta}_k))$:

$$\mathrm{dist}\big(\mathrm{CVAD}_i, p^{\mathrm{ref}}\big) \leq \frac{R_{\mathrm{w}} - V_{\mathrm{w}}}{2}, \tag{11}$$

where $\mathrm{dist}\big(\mathrm{CVAD}_i, p^{\mathrm{ref}}\big)$ is the Euclidean distance between current position of i-th vehicle and the point p^{ref}, with $i = 1, \dots, M$, R_{w} the road width, and V_{w} the vehicle width (see Figure 2).

3.5. Performance index

The performance index of the proposed optimization problem consists of J_{NMPCC} defined in Equation 5 and penalties on the control inputs computed for each CVAD in the plaza. Therefore, we define the performance index, at each sampling time k, as:

$$J = \sum_{i=1}^{M_k} \sum_{k=0}^{N-1} \left(\widehat{\boldsymbol{E}}_k^T Q \widehat{\boldsymbol{E}}_k + \boldsymbol{u}_k^T R \boldsymbol{u}_k + v_k^T \, r_{\mathrm{v}} v_k - q_\theta \hat{\theta}_k \right) \tag{12}$$

with M_k the total number of CVAD in the plaza at time step k and N the prediction horizon. The main reason to consider M_k as time-varying is that the vehicles continuously approach and leave the intersection. The elements on the diagonal of the control cost weight $R = \begin{bmatrix} r_{\mathrm{a}} & 0 \\ 0 & r_\delta \end{bmatrix}$ represent, respectively, the weights on the acceleration and steering angle rate of each vehicle, with $r_{\mathrm{a}} > 0$ and $r_\delta > 0$.

3.6. Optimal control problem

Combining the model, objective and constraints leads to the following optimal control problem:

$$\min_{\boldsymbol{u}} \sum_{i=1}^{M_k} \sum_{k=0}^{N-1} \left(\widehat{\boldsymbol{E}}_k^T Q \widehat{\boldsymbol{E}}_k + \boldsymbol{u}_k^T R \boldsymbol{u}_k + v_k^T \, r_{\mathrm{v}} v_k - q_\theta \hat{\theta}_k \right) \tag{13}$$

subject to Equation 8 and Equations 9, 10, and 11. The states and the control inputs of the problem are $\boldsymbol{z} = \left[x, y, \psi, v, \hat{\theta}\right]^T$ and $\boldsymbol{u} = [a, \delta, v]^T$, respectively. By tuning Q, q_θ, and r_v we can obtain a trade-off between contouring error, lag error, and approximated path progress. Furthermore, tuning R can affect the magnitude of control inputs. The problem in Equation 13 is a general nonlinear optimization problem that is converted to an NLP problem and solved online with respect to the current vehicles' states measured at each sampling time. Moreover, the predictions of the vehicles' states and control inputs are considered as decision variables whose optimal values are obtained using an NLP solver.

3.7. Continuous arrivals and solution algorithm

The main steps of the proposed E-NMPCC scheme are depicted in Figure 4. Based on intersection data, the reference paths between all possible origins and destinations in the plaza as well as the intersection boundaries are precomputed. This can be done by using interpolation techniques such as splines and the data of the centerline of each approach. The E-NMPCC algorithm is initialized by selecting appropriate values for the parameters such as prediction horizon, sampling time, weights, and safety distance.

The E-NMPCC algorithm starts by setting the time step $k = 0$. If there are no new arrivals and the network is empty, the time is incremented. Upon the arrival of the first vehicle, the NLP problem is instantiated and solved. After a solution is obtained, the states of the vehicles in the model are updated for the next step. The solution of the NLP provides the predictions of the vehicle states and control inputs for the next N time steps. However, the states are updated by only applying the first element of the predicted control inputs on the system. The time k is incremented. If there are vehicles that left or arrived at the intersection at the previous time step, a new instance of the problem in Equation 13 is created with the vehicles already in the intersection, with new arrivals and without the departed vehicles. In case there were no departures or new arrivals, the same NLP problem of the previous step is solved with updated states and initial conditions. This process continues until the intersection is empty, in which case the algorithm loops incrementing k until there is a new arrival. In this case, a new instance of the NLP is created and the optimization resumes.

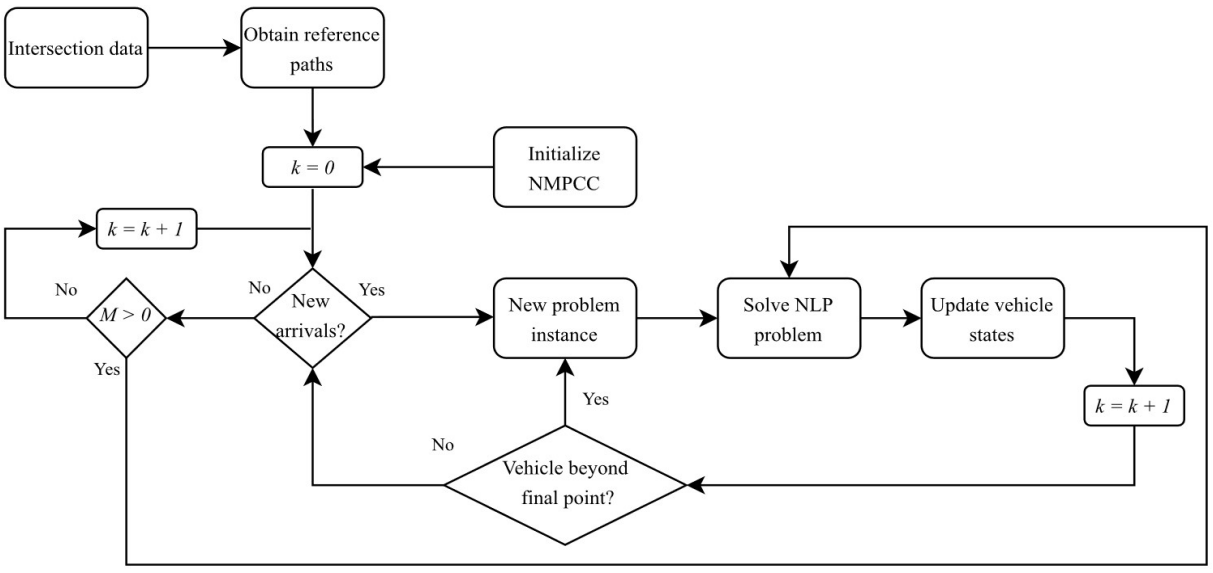


Figure 4: A flowchart of the E-NMPCC algorithm.

4. CASE STUDY SETUP AND RESULTS

In this section, we evaluate the proposed method for solving the problem in Equation 13 for CVAD at an urban intersection. The simulations are performed using Matlab R2018b equipped with CasADi, an open-source software package for nonlinear optimization and algorithmic differentiation (Andersson et al., 2019), to model the nonlinear optimal control problem 13. Moreover, to solve the corresponding NLP problem, we use the open-source IPOPT solver (Wächter and Biegler, 2006). The splines for obtaining the reference paths are computed using the Matlab *spline* command.

4.1. Scenario setup

A four-leg intersection depicted in Figure 2 is used for the simulations. There are two one-way intersecting roads, each of them has a through and a left or right turning movement. The CVAD randomly enter the plaza following a Poisson distribution, which describes the random occurrence of discrete events with an average arrival rate (Gerlough and Huber, 1976). In the first approach, the vehicles enter the plaza from the south and are allowed to either turn right or go straight. In the second approach, vehicles enter from the west and are allowed to either turn left or go straight. The four reference paths that could be followed by each CVAD according to the directions they enter and exit the plaza are shown in Figure 2. The initial position on the entering point and the initial speed of each CVAD are selected randomly using a uniform distribution. The initial speed of each CVAD is randomly selected between 2 to 4 m/s.

The final point at which the CVAD leave the plaza is chosen as $x = 60$ m or $y = 60$ m according to the used road. The other required parameters of the optimization problem, vehicles, and intersection are listed in Table 1. For this application, it is not necessary that the vehicles tightly follow the reference paths since the main priority is to maximize progress. Therefore, we choose low weights on the contouring error to give the vehicles freedom to move inside the plaza.

Table 1: Settings for vehicles, intersection, and optimization problem

Parameter	Description	Value	Unit
Δt	Sampling time	0.05	[s]
$v_{\max}$	Maximum speed	10	[m/s]
$u_{1,\max}$	Maximum acceleration	2	[m/s^2]
$u_{2,\max}$	Maximum steering angle	30	[deg/s]
f	Vehicle flow	1200	[veh/h]
d_{s}	Safe distance	0.5	[m]
l_{f}	Distance from CG to the front axle	1.10	[m]
l_{r}	Distance from CG to the rear axle	1.38	[m]
V_{w}	Vehicle width	1.7	[m]
L_{v}	Vehicle length	2.6	[m]
L_{w}	Lane width	10	[m]
Q	MPCC cost weight	diag(0.005, 5)	-
R_{u}	Control cost weight	diag(2, 0.5)	-
q_{θ}	Progress cost weight	2	-
r_{v}	Virtual input weight	0.02	-

N	Prediction horizon	15	-
M	Number of CVAD	10	-
n	Number of lanes	2	-

4.2. Analysis of the trajectories

The optimal and collision-free trajectories of CVAD generated by the solution of Equation 13 are illustrated in Figure 5. The figure shows a sequence of six snapshots of the proposed method. The time steps of the snapshots are 125, 155, 235, 275, 365, and 435. In the snapshots, the two black dashed lines show the reference paths for through movements, and the two light blue dotted lines show the reference paths for left and right turning. At each subfigure, we can see the trajectory of the vehicle until the snapshot time step by the colored solid line and its prediction for the next steps by the dotted lines of the same color. New arrivals are included in a new instance of the problem. For example, vehicle 4 (with red trajectory) from Figure 5(a) to Figure 5(b). Once the vehicle is beyond the final point, it is removed in the next instance of the problem, for example, vehicle 1 (with gray trajectory) from Figure 5(b) to Figure 5(c).

As can be seen in Figure 5, the vehicles are able to drive without being bound to the usual path-related road lanes and horizontal markings. Thus, the trajectories may deviate from what would be expected in a path-based method. The vehicles with the red, green, and purple trajectories in Figure 5(c) and the vehicle with the light blue trajectory in Figure 5(e) are suiting examples. The effectiveness of the collision avoidance constraint and the role of the prediction horizon can be seen in Figure 5(b). The green and purple vehicles were still in straight paths when a potential collision was predicted, as shown by the curved dotted lines in each predicted trajectory. The deviation is confirmed by the executed path seen in Figure 5(c).

To better assess the proposed method, Figures 6(a) to 6(e) show the speed, acceleration, orientation, steering angle, and progress profiles for six vehicles of interest (vehicles 2, 3, 5, 6, 8, and 9). To plot the figures, we assumed that vehicles have constant profiles, and thus, zero acceleration profiles before entering and after leaving the intersection plaza. Figure 6(f) shows the distances between six pairs of the vehicles of interest (vehicles 2-3, 2-4, 5-6, 7-8, 8-9, and 9-10). To plot the figure, we considered the time steps that every two vehicles are inside the intersection plaza.

To interpret the figures, we considered vehicles 2 and 3 as an example. Vehicle 3 is seen to reduce its speed and acceleration (Figures 6(a)-(b)). On the other hand, vehicle 2 is seen to increase its speed and acceleration (Figures 6(a)-(b)). Meanwhile both vehicles are seen to steer to the right and then to the left (Figure 6(c)) with corresponding temporary change in orientation (Figure 6(d)). Indeed, in Figure 5(c) one can see that vehicles 2 and 3 go further to the right relative to their previous position so that, along with the changes in speed (Figure 6(a)), a collision is avoided. It can be seen from Figure 6(e) that the distance between vehicles 2 and 3 (the green line) decreases and then increases staying above the minimum safe distance (the light blue line). Finally, in Figure 6(f), with the proposed method, all vehicles have increasing progress profiles, which is one of this paper's goals.

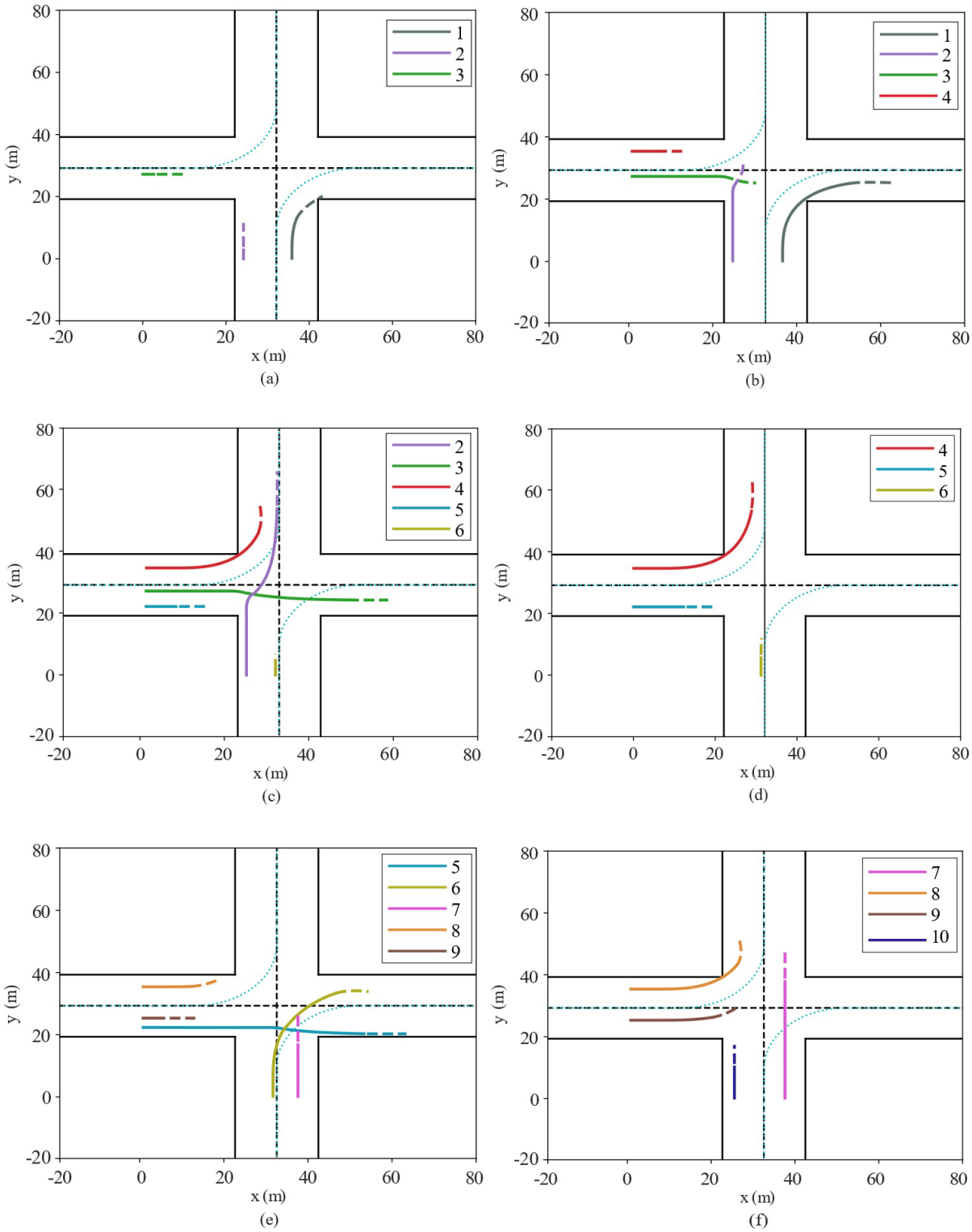


Figure 5: Snapshots of the trajectories of the vehicles at time steps 125, 155, 235, 275, 365, and 435 with a flow of 1200 veh/h per approach.

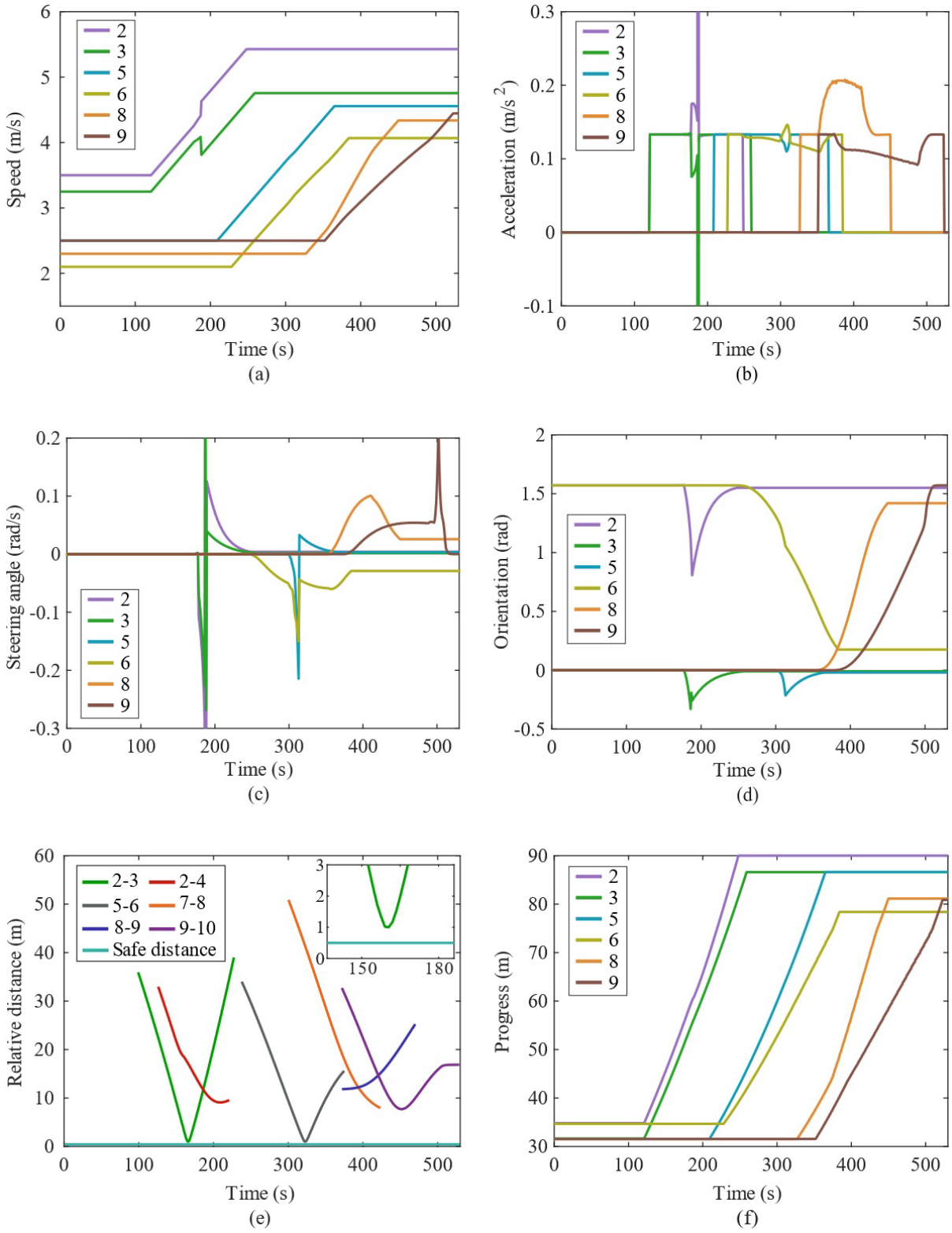


Figure 6. The state and control variables for six vehicles of interest (vehicles 2, 3, 5, 6, 8, and 9): (a) Speed; (b) acceleration; (c) steering angle; (d) orientation; (e) distance between every two selected vehicles; and (f) progress.

5. CONCLUSION

This paper presents a novel approach for solving the trajectory optimization problem for connected vehicles under automated driving (CVAD) in the free use of the intersection

space, using the nonlinear model predictive contouring control (NMPCC) approach. The proposed method extended the standard NMPCC (Lam, Manzie and Good, 2010) by incorporating multiple reference paths according to the vehicle's intention of traversing the intersection and by working with loose contouring error. Thus, optimal, collision-free, and path-free trajectories were generated for the CVAD. The simulation results showcased the effectiveness of the extended NMPCC (E-NMPCC) in solving the intersection trajectory optimization problem under scenarios with continuous arrivals of vehicles.

The average computation time for generating trajectories in the studied scenario is 1.31 seconds per time step. This is because the real-time solution of the formulated optimization problem, which deals with vehicle-to-vehicle collision avoidance constraints, is computationally expensive due to the nonlinearity and non-convexity of these constraints. To further enhance the method's capabilities, ongoing investigations are focusing on refining the solution process of the optimal control problem. These enhancements aim to expedite the trajectory generation and decision-making process, making it more applicable in real world. Tests in a laboratory setting as done by Levy and Haddad (2022) for a road without lanes should, however, precede real-world testing and are envisaged as future work. Communication between vehicles and infrastructure were assumed perfect. Modeling of communication should be incorporated into the problem (Sarker et al., 2020). Future work in this domain should encompass a comparative analysis with other path-based methods as done by Carlson et al. (2022). Such a comparison should evaluate the performance of these methods using standard traffic performance metrics, including traffic delay and intersection capacity. In addition, it is imperative to consider constraints that guarantee passenger comfort during the trajectory optimization process. Future research should take into account passenger comfort and assess its impact on trajectory optimization algorithms (Le Vine, Zolfaghari and Polak, 2015).

ACKNOWLEDGEMENTS

This work was supported by The Brazilian Agency for Higher Education (CAPES), under the project PrInt CAPES-UFSC "Automation 4.0"' and with a doctorate student scholarship; by the National Council for Scientific and Technological Development (CNPq) under grants 304555/2020-7 and 422481/2021-1; and by FAPESC under grant 2021TR001851.

REFERENCES

Ahmadi, E. and R.C. Carlson (2022) Model predictive control of multi-vehicle interaction at unsignalized intersections. In *36º ANPET-Congresso de Pesquisa e Ensino em Transportes.* Rio de Janeiro: ANPET, p. 1-12.

Ahmadi, E.; R.C. Carlson; W. Kraus Jr et al. (2021) Near-optimal coordination of vehicles at an intersection plaza using finite fourier series. In *35º ANPET-Congresso de Pesquisa e Ensino em Transportes*. Rio de Janeiro: ANPET, p. 2458-2469.

Ahmadi, E.; R.C. Carlson; W. Kraus Jr et al. (2022) Near-optimal coordination of vehicles at an intersection plaza using bézier curves. In *The Eleventh International Conference on Advances in Vehicular Systems, Technologies and Applications*, Venice: IARIA, p. 6-12.

Amouzadi, M.; M.O. Orisatoki and A.M. Dizqah (2022) Optimal lane-free crossing of cavs through intersections. In *IEEE Transactions on Vehicular Technology,* New York: IEEE, p. 1488-1500. DOI: 10.1109/TVT.2022.3207054

Andersson, J.A.; J. Gillis; G. Horn et al. (2019) CasADi: a software framework for nonlinear optimization and optimal control, *Mathematical Programming Computation*, v. 11, n. 1, p. 1-36. DOI: 10.1007/s12532-018-0139-4.

Carlson, R.C.; E. Ahmadi; E.R. Müller et al. (2022) Optimal coordination of connected vehicles under automated driving at path-free signal-free urban intersections. In *36º ANPET-Congresso de Pesquisa e Ensino em Transportes.* Rio de Janeiro: ANPET, p. 1-12.

Chen, L. and C. Englund (2015) Cooperative intersection management: a survey, *IEEE Transactions on Intelligent Transportation Systems*, v. 17, n. 2, p. 570-86. DOI: 10.1109/TITS.2015.2471812.

Faulwasser, T.; B. Kern and R. Findeisen (2009) Model predictive path-following for constrained nonlinear systems. In *Proceedings of the 48h IEEE Conference on Decision and Control (CDC) held jointly with 2009 28th Chinese Control Conference*. New York: IEEE, p. 8642-8647. DOI: 10.1109/CDC.2009.5399744.

Gerlough, D.L. and M.J. Huber (1976) Traffic flow theory, *Transp. Res. Board Special Rep*, v. 165, p. 222.

Lam, D.; C. Manzie and M. Good (2010) Model predictive contouring control. In *49th IEEE Conference on Decision and Control (CDC)*. New York: IEEE, p. 6137-6142. DOI: 10.1109/CDC.2010.5717042.

Le Vine, S.; A. Zolfaghari and J. Polak (2015) Autonomous cars: the tension between occupant experience and intersection capacity, *Transportation Research Part C, Emerging Technologies*, v. 52, p. 1-14. DOI: 10.1016/j.trc.2015.01.002.

Lee, J. and B. Park (2012) Development and evaluation of a cooperative vehicle intersection control algorithm under the connected vehicles environment, *IEEE Transactions on Intelligent Transportation Systems*, v. 13, n. 1, p. 81-90. DOI: 10.1109/TITS.2011.2178836.

Levy, R. and J. Haddad (2021) Path and trajectory planning for autonomous vehicles on roads without lanes. In *IEEE International Intelligent Transportation Systems Conference (ITSC)*. New York: IEEE, p. 3871-3876. DOI: 10.1109/ITSC48978.2021.9565023.

Levy, R. and J. Haddad (2022) Cooperative path and trajectory planning for autonomous vehicles on roads without lanes: a laboratory experimental demonstration, *Transportation Research Part C, Emerging Technologies*, v. 144, p. 103813. DOI: 10.1016/j.trc.2022.103813.

Li, B.; Y. Zhang; N. Jia et al. (2020) Autonomous intersection management over continuous space: a microscopic and precise solution via computational optimal control, *IFAC-PapersOnLine*, v. 53, n. 2, p. 17071-6. DOI: 10.1016/j.ifacol.2020.12.1611.

Li, B.; Y. Zhang; T. Acarman et al. (2021) Lane-free autonomous intersection management: a batch-processing framework integrating reservation-based and planning-based methods. In *IEEE International Conference on Robotics and Automation (ICRA).* New York: IEEE, p. 7915-7921. DOI: 10.1109/ICRA48506.2021.9562015.

Li, B.; Y. Zhang; Y. Zhang et al. (2018) Near-optimal online motion planning of connected and automated vehicles at a signal-free and lane-free intersection. In *2018 IEEE Intelligent Vehicles Symposium (IV)*. New York: IEEE, p. 1432-1437. DOI: 10.1109/IVS.2018.8500528.

Liniger, A.; A. Domahidi and M. Morari (2015) Optimization-based autonomous racing of 1: 43 Scale RC Cars, *Optimal Control Applications & Methods*, v. 36, n. 5, p. 628-47. DOI: 10.1002/oca.2123.

Müller, E.R.; R.C. Carlson and W. Kraus Jr (2016a) Intersection control for automated vehicles with MILP, *IFAC-PapersOnLine*, v. 49, n. 3, p. 37-42. DOI: 10.1016/j.ifacol.2016.07.007.

Müller, E.R.; R.C. Carlson and W. Kraus Jr (2016b) Time Optimal Scheduling of Automated Vehicle Arrivals at Urban Intersections. In *IEEE 19th International Conference on Intelligent Transportation Systems (ITSC)*. New York: IEEE, p. 1174-1179. DOI: 10.1109/ITSC.2016.7795705.

Papageorgiou, M.; K.S. Mountakis; I. Karafyllis et al. (2021) Lane-free artificial-fluid concept for vehicular traffic, *Proceedings of the IEEE*, v. 109, n. 2, p. 114-21. DOI: 10.1109/JPROC.2020.3042681.

Polack, P.; F. Altché; B. d'Andréa-Novel et al. (2017) The kinematic bicycle model: a consistent model for planning feasible trajectories for autonomous vehicles? In *IEEE Intelligent Vehicles Symposium (IV)*, New York: IEEE, p. 812-818. DOI: 10.1109/IVS.2017.7995816.

Rios-Torres, J. and A.A. Malikopoulos (2016) A survey on the coordination of connected and automated vehicles at intersections and merging at highway on-ramps, *IEEE Transactions on Intelligent Transportation Systems*, v. 18, n. 5, p. 1066-77. DOI: 10.1109/TITS.2016.2600504.

Romero, A.; S. Sun; P. Foehn et al. (2022) Model predictive contouring control for time-optimal quadrotor flight, *IEEE Transactions on Robotics*, v. 38, n. 6, p. 3340-56. DOI: 10.1109/TRO.2022.3173711.

Rossiter, J. (2018) *A First Course in Predictive Control*. London: CRC press.

Sarker, A.; H. Shen; M. Rahman et al. (2020) A review of sensing and communication, human factors, and controller aspects for information-aware connected and automated vehicles, *IEEE Transactions on Intelligent Transportation Systems*, v. 21, n. 1, p. 7-29. DOI: 10.1109/TITS.2019.2892399.

Schepperle, H. and K. Böhm (2009) Valuation-aware traffic control: the notion and the issues. In Bazzan, A. and F. Klügl (eds.) *Multi-Agent Systems for Traffic and Transportation Engineering*, Hershey: IGI Global, p. 22. DOI: 10.4018/978-1-60566-226-8.ch010.

Schwarting, W.; J. Alonso-Mora; L. Paull et al. (2017) Safe nonlinear trajectory generation for parallel autonomy with a dynamic vehicle model, *IEEE Transactions on Intelligent Transportation Systems*, v. 19, n. 9, p. 2994-3008. DOI: 10.1109/TITS.2017.2771351.

Wächter, A. and L.T. Biegler (2006) On the implementation of an interior-point filter line-search algorithm for large-scale nonlinear programming, *Mathematical Programming*, v. 106, n. 1, p. 25-57. DOI: 10.1007/s10107-004-0559-y.